

# Fully Automatic Skull-Stripping in 3D Time-of-Flight MRA Image Sequences

N. D. Forkert<sup>1</sup>, D. Säring<sup>1</sup>, J. Fiehler<sup>2</sup>, T. Illies<sup>2</sup>, M. Färber<sup>1</sup>, D. Möller<sup>3</sup> and H. Handels<sup>1</sup>

<sup>1</sup>Department of Medical Informatics, University Medical Center Hamburg-Eppendorf, Germany

<sup>2</sup>Department of Diagnostic and Interventional Neuroradiology, University Medical Center Hamburg-Eppendorf, Germany

<sup>3</sup>Department Computer Engineering, Faculty of Mathematics, Informatics and Natural Sciences, University of Hamburg, Germany

---

## Abstract

*In this paper we present a robust skull-stripping method for the isolation of cerebral tissue in 3D Time-of-Flight (TOF) magnetic resonance angiographic images of the brain. 3D TOF images are often acquired in case of cerebral vascular diseases, because of their good blood-to-background-contrast. Skull-stripping is an essential preprocessing step towards a better segmentation as well as direct visualization of the vascular system. Our approach consists of three main steps. After preprocessing in order to reduce signal inhomogeneities and noise the first main step is the segmentation of the surrounding skull using a region growing approach. The second step is the automatic extraction of distinctive points at the border of the brain, based on the segmentation of the skull, which are then used as supporting points for a graph based contour extraction. The third step is a slicewise correction based on a non-linear registration in order to improve sub-optimal segmentation results. The method proposed was validated using 18 manually stripped datasets. The calculated similarity measures show that the proposed method leads to good segmentation results with only a few segmentation errors. At the same time the mean rate of vessel voxels included by the brain segmentation is 99.18%. In summary the procedure suggested allows a fast and fully automatic segmentation of the brain and is especially helpful as a preprocessing step towards an automatic segmentation of the vessel system or direct volume rendering.*

Categories and Subject Descriptors (according to ACM CCS): I.4.6 [Image Processing and Computer Vision]: Segmentation

---

## 1. Introduction

Many people suffer from cerebral vascular diseases like aneurysms or arteriovenous malformations (AVM). These may lead to strokes if not diagnosed in time. Three-dimensional time-of-flight (TOF) MR angiography is the most commonly used non invasive method for evaluating the intracranial vasculature [DWH\*93]. TOF MRA image sequences offer a high spatial resolution and a superior blood-to-background-contrast. Thus, a detailed segmentation of the vessel system is possible. A detailed knowledge about the individual anatomy of the cerebral vessel system is needed for correct diagnosis and planning of an endovascular treatment. Therefore the segmentation or direct visualization of the vessel system is an important step towards an improved therapy.

This work is part of a project dealing with visualization and quantitative analysis of cerebral arteriovenous malformations. Spatiotemporal 4D magnetic resonance angiography (MRA) image datasets and 3D MRA datasets with high spatial resolution are used for analyzing AVMs. One of the main tasks is the combination of the information of these 3D and 4D MRA image sequences to support the evaluation of the AVM. The segmentation of the vessel system is the main prerequisite for this analysis [SFF\*07].

In spite of the high number of publications dealing with cerebrovascular segmentation, it is still a challenging problem. Current approaches often suffer from oversegmentation of non-cerebral tissue classes like fat, bone marrow and eyes due to the similar intensity distribution and connections to the vessel system. Especially stochastic approaches that are only based on the given image intensities as described

in [WN99], [HFHM06] and [CSP04] are affected by this problem. Direct volume rendering techniques suffer from a similar problem as the vessels are hidden by non-brain tissues (especially skin and fat structures). An initial isolation of the brain tissue from extracranial tissues, often referred to as skull-stripping or skull-peeling, is therefore a fundamental preprocessing step towards a better segmentation or direct volume rendering of the vascular system. Furthermore regional volume calculations of brain tissue are useful for diagnostics of cerebrovascular diseases. The segmentation of the brain may also serve as a preprocessing step for atlas-based registration methods, since some registration algorithms perform differently (e.g. nonlinear warping) on stripped and unstripped data [RSA\*04]. The segmentation of the brain is therefore not only essential for accurately detecting and visualizing vessels of the brain, but it also provides several other benefits.

Numerous skull-stripping methods have been proposed. Fennema-Nostine et al. [FN\*06] published a quantitative evaluation of four automated skull-stripping (3dIntracranial, Brain Extraction Tool [Smi02], Hybrid Watershed Algorithm [SDB\*04] and Brain Surface Extractor [SSLS\*01]) methods in 2006. Legacy and contemporary T1-weighted image sets were used as input. For evaluation two anatomists manually segmented the brain in six sagittal slices from each raw MR image set. They pointed out that the performance of these methods, which rely on signal intensity and signal contrast may be influenced by numerous factors including MR signal inhomogeneities, type of MR image set, gradient performances, stability of system electronics and extent of neurodegeneration. Segmentation errors might lead to time consuming manual postprocessing.

We tested the free available software for skull-stripping Free-Surfer [DFS99], Brain Extraction Tool [Smi02] and Brain Surface Extractor [SSLS\*01] with TOF image sequences as input. The tested methods lead to segmentation errors, when applied to the TOF-MRA. The vessels, which are represented by a high intensity distribution, are a problematic structure for the established methods, often leading to undersegmentation. Leaking to non-brain tissues, because of strong connections between the brain and non-brain tissues (Fig. 1), was another problem resulting in an oversegmentation. Skull-stripping methods which focus especially on 3D-TOF image sequences are not known to the authors.

In this work we propose a novel skull stripping method, which takes into account the specific characteristics of TOF-datasets. Initially, preprocessing is applied to the TOF-dataset in order to reduce signal inhomogeneities and noise. In a next step the skull, which surrounds the brain, is roughly segmented using region growing. Then, based on this segmentation, distinctive points at the border of the brain are extracted automatically. These points are used as supporting points for a graph based contour extraction. Slicewise correction, based on a non-linear registration, is applied if needed in order to reduce sub-optimal segmentation results. The main challenge was to eliminate non-brain voxels,

which are represented by similar intensities like vessels tissues, while all vessel voxels should be included by the segmentation at the same time.

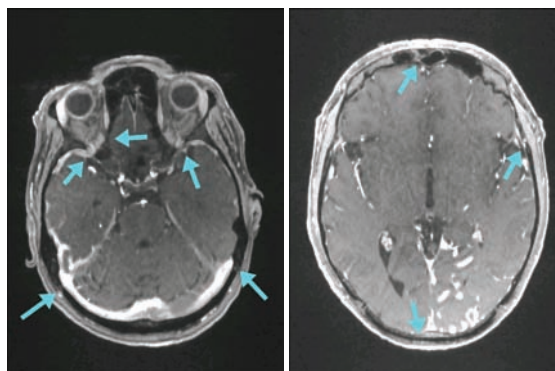


**Figure 1:** Problematic structures for established brain stripping methods marked by arrows two slices from a TOF-MRA image sequence.

## 2. Material and Methods

### 2.1. Material

For development and evaluation of the automatic brain segmentation method 18 datasets were available. The MRI measurements were carried out on a 3T Trio scanner (Siemens, Erlangen, Germany) using an 8-channel-phased array-head-coil. The 3D TOF images were obtained after application of a contrast agent with a magnetization transfer saturation (MTS) pulse, TR 36 ms, TE 6 ms, flip angle  $25^\circ$ , 5 slabs with 40 partitions, image in-plane image resolution of 0.47 mm x 0.47 mm, slice thickness 0.5 mm, and a FOV of 150 mm x 200 mm. After a device-related preprocessing of the slabs each dataset consists of 156 slices.

### 2.2. Preprocessing

The Time-of-Flight datasets are acquired via a multi-slab technology. Unfortunately this results in slice-to-slice amplitude variations associated with imperfect slab definitions [LXL00]. Therefore neighbouring slabs are measured with a lap of 20 to 30 % in order to compensate these variations of the amplitudes. The neighbouring slabs are then combined mathematically after acquisition. Despite the device-related preprocessing a reduction of the amplitude can be observed in the overlapping region. This might lead to unwanted results during further intensity based processing steps at the slab boundary. This phenomenon is often referred to as slab boundary artifact (SBA). In order to reduce these intensity inhomogeneities the method proposed by Kholmovski et al. [KAP02] is used.

After correction of the slab boundary artifact the in-slice bias fields are corrected using the proposed method by Styner et

al. [SGBS00]. Finally an anisotropic smoothing is applied in order to reduce strong noise in the data [WX01].

### 2.3. Initial Segmentation of the Skull

Initially the skull is segmented slicewise using a 2D region growing. The slice individual upper threshold for the region growing can be extracted from the intensity histogram using an adapted method proposed by Hassouna et al. [HFHM06]. For this purpose each TOF-slice histogram was divided into two regions based on voxel intensity. A Rayleigh distribution is used to model the lower intensity region, which corresponds to the skull and background, while a Gauss distribution is used to model the higher intensity region, which corresponds to the remaining tissues like eyes, fat, vessels and brain. Those distributions are used by a mixture model to characterize the intensity distribution of the slice, whereas the parameters are estimated using the expectation maximization (EM) algorithm. After an appropriate mixture model is computed, the threshold can be defined in terms of minimum error classification. The seed points for the region growing can be extracted by a line- respectively columnwise analysis of the intensity profile in each slice where the skull is represented by a dip (Fig. 2).

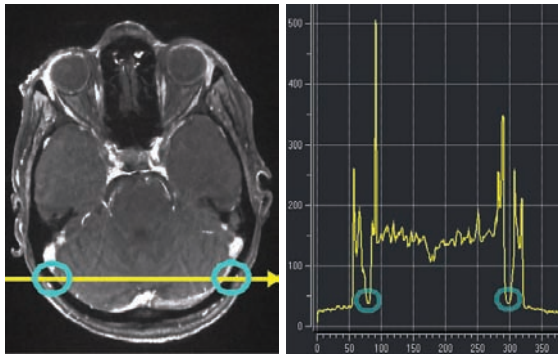


**Figure 2:** TOF MRA slice (left), intensity profile of the yellow line displayed in the left figure (right).

### 2.4. Graph based Skull Stripping

A closed contour of the brain can not yet be extracted from this initial automatic segmentation since the brain appears to be not totally surrounded by the skull in the TOF image sequences. In order to generate the closed contour needed we initially extract supporting points out of the initial segmentation which are then connected using a graph based approach.

#### 2.4.1. Extraction of Supporting Points

In order to extract the supporting points needed, the center of gravity of the segmented skull in the TOF-Slice is calculated. Then rays are computed with a distance of 18 degrees

starting from the center of gravity. For each two neighbouring rays the segmented pixel within the spanned area with the least distance to the center of gravity is identified. In doing so 20 distinctive points at the border between the brain and the skull are extracted for the graph based contour search in each slice (Fig. 3). A following analysis of the extracted supporting points is used to exclude outliers which are represented by a high distance difference to the center of gravity compared to their direct neighbors.

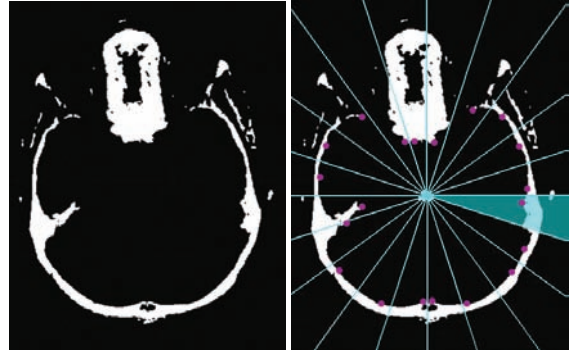


**Figure 3:** Result of the Region-Growing (left), Rays and extracted supporting points (purple) within the spanned area of each two rays (right)

#### 2.4.2. Graph based Connection of Distinctive Points

The proposed graph-based contour extraction is based on the 2D live-wire method [BM97]. The live-wire segmentation approach formulates the problem of creating the boundary of medical structures as a path-searching problem in a cost weighted graph. The basic idea is to find the cost optimal path between a start and a goal node. If the edges of the structure are well defined, these paths will align to its outline and form the segmentation result.

The pixels of an image  $f_I$  of size  $n \times m$  are represented as graph nodes and edges are created between each pixel and its eight neighbors. The cost optimal path is then defined as the path with minimal costs concerning the sum of the local costs of each edge visited on the path from start to goal node. The 2D live-wire method used in this study uses the gradient magnitude  $f_{GM}$ , gradient direction  $f_{GD}$  and Deriche edge detection [Der87]  $f_{DE}$  as cost terms. They are combined in a weighted sum to form the costs of an edge  $c(p,q)$  between the nodes  $p$  and  $q$ .

$$c(p, q) = \omega_{GM} f_{GM}(q) + \omega_{GD} f_{GD}(p, q) + \omega_{DE} f_{DE}(q) \quad (1)$$

The weight constants  $\omega_{GM}$ ,  $\omega_{GD}$  and  $\omega_{DE}$  allow each cost term to contribute to the cost function at different rates. The cost term for the gradient magnitude is defined as

$$f_{GM} = 1 - \sqrt{\left(\frac{df_I}{dx}\right)^2 + \left(\frac{df_I}{dy}\right)^2} / \max G \quad (2)$$

where  $\max G$  is the highest gradient magnitude in the 2D image. Since the live-wire algorithm searches for the path with the minimum cost the gradient magnitude must be inverted. The gradient direction cost term contributes a smoothness constraint by assigning high costs to sharp changes. The gradient direction cost term for pixel  $p$  going to pixel  $q$  is defined as

$$f_{GD}(p, q) = \operatorname{acos} \left( \frac{\left. \frac{df_i}{dx} \right|_p}{G(p)} \times \frac{\left. \frac{df_i}{dx} \right|_q}{G(q)} + \frac{\left. \frac{df_i}{dy} \right|_p}{G(p)} \times \frac{\left. \frac{df_i}{dy} \right|_q}{G(q)} \right) / \pi \quad (3)$$

where  $G(p)$  represents the gradient magnitude for pixel  $p$ . The Deriche edge detection filter is based on recursive filtering, hysteresis thresholding and edge tracking mechanisms and replaces the Laplacian zero crossing feature that is used in the original live-wire approach. This edge detection filter is more robust against noise and the edges detected are fine and continuous.

The empirical determined values for these weight constants used in this work are  $\omega_{GM} = 0.4$ ,  $\omega_{GD} = 0.8$  and  $\omega_{DE} = 0.2$ . Given the start pixel (seed point  $S$ ) a dynamic programming method [Dij59] is used to calculate the minimum spanning tree with root  $S$ . The complexity of building the minimum spanning tree for an image of size  $n \times m$  pixels is of  $O(n \times m)$ . The minimum spanning tree includes the minimum cost paths from  $S$  to all image pixels.

Starting from an initial distinctive point  $p$  the cost optimal path between this point and its neighbour in clockwise direction  $q$  is computed using the described graph search approach. After the cost optimal path is computed the distinctive point  $q$  is set to  $p$  and its next neighbor to  $q$ . The contour is closed if the initial distinctive point is reached again. By iteratively performing this operation, the closed contour of the brain is extracted for each slice (Fig. 4).

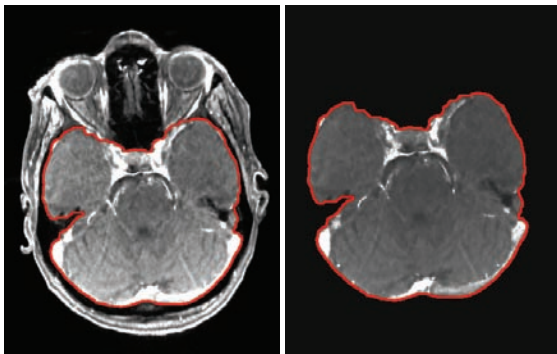


**Figure 4:** TOF MRA slice with red displayed brain contour (left), the TOF slice masked with the computed brain segmentation (right).

## 2.5. Contour-Analysis and Postprocessing

The biggest advantage of the automatic graph based approach used to segment the brain is that it cuts through tissue if this is the cost optimal path. This is especially helpful in case of the eyes where most other approaches lead to segmentation errors in terms of leaking to non-brain tissue. This advantage also has its drawbacks. It may cause unwanted clipping of brain tissue in other areas of the brain, especially if there is a low signal contrast between the bone structures of the skull and the brain tissue. Incorrect distinctive points are also a problem which may lead to false contours (Fig. 5). Based on the assumption that the visual content of two neighbouring slices does not vary too much, due to the small slice thickness, it can be assumed that the brain segmentations of two neighbouring slices do not vary strongly. For comparison of two neighbouring segmentations  $A$  and  $B$  the automatically extracted contours are binarized and the Tanimoto coefficient (also known as the Jacquard coefficient):

$$T(A, B) = \frac{|A \cup B|}{|A \cap B|} \quad (4)$$

is calculated. Values close to 1 indicate a good consensus, whereas values close to 0 indicate a bad consensus.

The main idea behind the postprocessing is to identify slices with a segmentation which differs significantly from its neighbouring slice. Those slices are replaced by an interpolated segmentation based on a non-linear registration method.

In order to define a starting slice for the slicewise comparison a slice with a good segmentation must be identified. For this purpose the Tanimoto coefficient is calculated for every neighbouring slices. Then the slice with the highest mean Tanimoto coefficient over 6 slices is identified and defined as the initial reference slice  $S_i$ .

Starting from this reference slice we compare the next neighbouring segmentation slice  $S_{\hat{i}}$  ( $\hat{i} = i - 1$  respectively  $\hat{i} = i + 1$ ) in  $z$ -direction. If the Tanimoto coefficient is above a defined threshold  $\theta$  (in this work we used a threshold of  $\theta = 0.97$ ) the neighbouring slice is set to  $S_i$ . If the Tanimoto coefficient is below this threshold we compute the displacement field  $\varphi$  between the TOF-slice reference image  $T_i$  which corresponds to  $S_i$  and the TOF-slice  $T_{\hat{i}}$  which corresponds to  $S_{\hat{i}}$ . The non-rigid 2D-2D registration used in this work follows the demons algorithm proposed by Thirion [Thi98]. The displacement field  $\varphi$  is computed such that

$$T_{\hat{i}} = \varphi \circ T_i \quad (5)$$

Then  $S_{\hat{i}}$  is transformed using  $\varphi$ . For reduction of interpolation artifacts morphological erosion followed by dilation is applied. In this work a kernel size of 5 turned out to yield adequate results. The resulting image is then used as a new reference slice.

Beginning from the initial reference slice this procedure is carried out in both directions on the complete dataset.

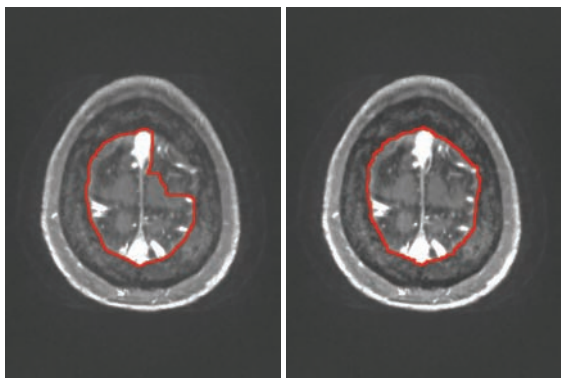


**Figure 5:** TOF MRA slice with red displayed brain contour (left), the TOF slice with red displayed brain contour after postprocessing (right).

### 3. Results

The described method for skull stripping was developed in C++ based on the open insight segmentation and registration toolkit (ITK) and the open visualization toolkit (VTK). For the development and evaluation 18 datasets were available. For evaluation purposes for every dataset the brain was manually segmented by medical experts.

For each dataset the automatic computed segmentation  $A$  was compared to the manual segmentation  $M$  for evaluation of the automatically computed brain stripping.

The Dice coefficient  $D(A, M)$ , Tanimoto coefficient  $T(A, M)$  and Hausdorff distance  $H(A, M)$  were used as empirical similarity measures to evaluate the segmentation results.

The Dice coefficient  $D(A, M)$  is defined by:

$$D(A, M) = \frac{2|A \cap M|}{|A| + |M|} \quad (6)$$

Like the Tanimoto coefficient (4) values close to 1 indicate a good consensus, whereas values close to 0 indicate a bad consensus.

The Hausdorff distance  $H(A, M)$  measures the maximal distance between the surfaces of two segmentations and is defined by

$$H(A, M) = \max \{h(A, M), h(M, A)\} \quad (7)$$

with

$$h(A, M) = \max_{a \in A} \min_{m \in M} d(a, m) \quad (8)$$

whereas  $A$  and  $M$  represent the set of points of the two surfaces and  $d(a, m)$  the distance between two points. Low values indicate a good consensus.

The Dice coefficient, Tanimoto coefficient and Hausdorff distance measure the global similarity. Little differences between two segmentations at the border area do not lead to strong changes of this similarity measures. Vessels often occur at the border area of the brain. Since it is one of the main

task of the proposed method to serve as a preprocessing step for vessel segmentation all vessels should be included in the brain segmentation. Since the similarities measures introduced above do not provide information about how good the automatic brain segmentation includes the vessel system we introduce a specific measure to quantify the inclusion rate of vessel voxels by the automatic segmentation of the brain.

The vessel system was segmented semi-automatically by medical experts using thresholding techniques and a region-growing algorithm with subsequent manual correction in the orthogonal views of the 3D TOF MRA. As an application-specific coefficient  $I(A, V)$  the percentage of segmented vessel voxels of the semi-automatic segmentation  $V$  included by the automatic brain segmentation  $A$  was determined:

$$I(A, V) = 100 \frac{|A \cup V|}{|V|} \quad (9)$$

Table 1. shows the results of this quantification for the 18 datasets used.

Dataset	$D(A, M)$	$T(A, M)$	$H(A, M)$	$I(A, V)$
01	0.970	0.985	15.74	99.54%
02	0.971	0.985	09.76	99.38%
03	0.975	0.987	14.60	99.01%
04	0.976	0.988	11.60	99.57%
05	0.949	0.974	22.72	99.42%
06	0.981	0.991	11.59	99.91%
07	0.986	0.993	07.28	99.81%
08	0.981	0.991	10.04	99.38%
09	0.959	0.979	20.44	98.74%
10	0.975	0.988	10.32	99.43%
11	0.969	0.984	11.92	97.22%
12	0.969	0.984	09.48	99.92%
13	0.939	0.969	22.97	97.94%
14	0.987	0.993	04.17	99.50%
15	0.979	0.989	09.04	99.28%
16	0.981	0.991	11.07	99.74%
17	0.982	0.991	11.64	99.78%
18	0.954	0.976	16.85	97.75%
mean	0.971	0.985	12.85	99.18%
SEM	0.013	0.007	5.20	0.72%

**Table 1:** Results of the evaluation of the proposed skull-stripping method for 18 datasets and the calculated means and standard errors of the means (SEM).

The calculated similarity measures show that the proposed method leads to segmentation results with only a few segmentation errors. The good quantitative results were also confirmed via visual rating by medical experts.

The manual segmentation of the brain took 2.5 hours in average per dataset. The computation time needed for the automatic brain segmentation averaged out to 30 minutes.

#### 4. Conclusion

The proposed method is able to segment the brain tissue fully automatically. Because the live-wire approach is used to initially segment the brain, the described method allows robust results even in case of strong connections between the brain and neighbouring tissues.

The mean inclusion rate of 99.18% of vessel voxels by the automatic brain segmentation and the good quantitative similarity measures show that the main goal of this method to serve as a preprocessing step towards a better segmentation of the vessel system was achieved. Problematic structures for the vessel segmentation like bone marrow, optical nerves and eyes are excluded while nearly all vessel voxels inside the brain were included in the stripped brain.

Fig. 6 and 7 show the same TOF image sequence volume rendered using the same transfer function. Fig. 6 shows the unstripped and Fig. 7 the automatically stripped volume. It becomes apparent that the vessels are displayed much better using the stripped volume since disturbing non-brain tissues are excluded. The stripped TOF-image sequence allows in contrast to the unstripped dataset a fast and direct visualization of the cerebral vessel structure.

The interaction time for the manual post-editing only takes a few minutes in contrast to the 2.5 hours needed for the manual segmentation. The few segmentation errors can be ascribed to weak edges on the border of the brain, resulting in a slight oversegmentation at some parts of the skull. A following segmentation or direct visualization of the vessel system will not be affected by this oversegmentation because of the low intensities.

In the publication by Fennema-Nostine et al. [FN\*06] among others the Tanimoto coefficient (Jacquard coefficient) and the Hausdorff distance were used as empirical similarity measures for evaluation of automatic segmentation results. The four methods evaluated achieved a mean Tanimoto coefficient from 0.787 to 0.865 and a mean Hausdorff distance from 26.2 to 14.6. Although this results can not be transferred directly to the TOF MRA (also T1-weighted) used in this study they reflect the impression of the visual rating of the results yielded by Free-Surfer, Brain Extraction Tool and Brain Surface Extractor when using the TOF as input.

The few segmentation errors can be ascribed to weak edges at the border of the brain tissues. Especially bone marrow leads to local oversegmentations, which have little impact on the tanimoto coefficient used in the postprocessing step and are therefore not corrected. Hence it is planned to replace the global detection of segmentation errors by a more local detection.

Further improvements of the segmentation results might be achieved by including other image sequences, like a T1-weighted scan, into the proposed method.

Although the average time of 30 minutes needed for the automatic brain segmentation is within the scope of the given clinical requirements, there is still potential for acceleration. Since the postprocessing is the most time consuming step,

the proposed method could be accelerated by identifying subregions with possible segmentation errors first and performing the non-linear registration only on those subregions. For further evaluation of the proposed method we are planning to quantitative compare the results of the proposed segmentation method to those yielded by other approaches. Furthermore we intend to apply our approach to different image sequences in order to evaluate the broad applicability of the technique.

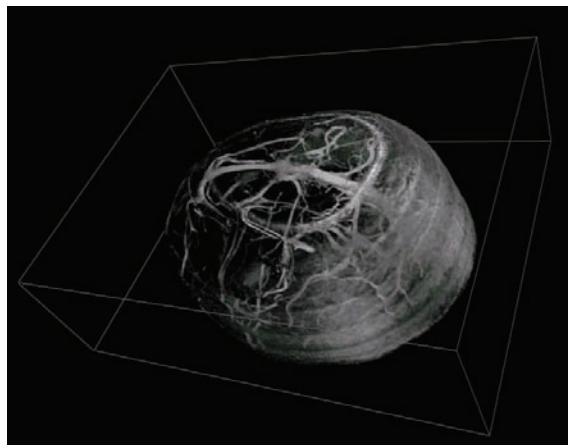


**Figure 6:** Volume rendered TOF MRA dataset.

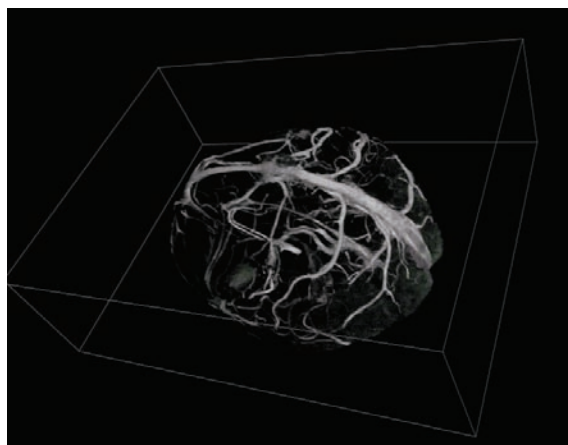


**Figure 7:** The same TOF MRA dataset volume as in Figure 6 but masked with the automatic extracted brain segmentation rendered with the same transfer function

**Acknowledgments:** This work is supported by German Research Foundation (DFG, HA 2355/10-1).

## References

- [BM97] BARRET W., MORTENSEN E.: Interactive live-wire boundary extraction. *Medical Image Analysis* 1, 4 (1997), 331–341.
- [CSP04] CHAPMAN B., STAPELTON J., PARKER D.: Intracranial vessel segmentation from time-of-flight mra using pre-processing of the mip z-buffer: accuracy of the zbs algorithm. *medical Image Analysis* 8, 2 (Jun 2004), 113–126.
- [Der87] DERICHE R.: Using canny’s criteria to derive a recursively implemented optimal edge detector. *Internat. J. Vision* 1, 2 (1987), 167–187.
- [DFS99] DALE A., FISCHL B., SERENO M.: Cortical surface-based analysis i segmentation and surface reconstruction. *Neuroimage* 9 (1999), 179–194.
- [Dij59] DIJKSTRA E.: A note on two problems in connexion with graphs. *Numerische Mathematik* 1 (1959), 269–271.
- [DWH\*93] DAVIS W., WARNOCK S., HARNSBERGER H., PARKER D., CHEN C.: Intracranial mra: single volume vs. multiple thin slab 3d time-of-flight acquisition. *J Comput Assist Tomogr.* 17, 1 (Jan-Feb 1993), 15–21.
- [FN\*06] FENNEMA-NOSTINE C., ET AL.: Quantitative evaluation of automated skull-stripping methods applied to contemporary and legacy images: Effects of diagnosis, bias correction, and slice location. *Human Brain Mapping* 27, 2 (Feb 2006), 99–113.
- [HFHM06] HASSOUNA M. S., FARAG A., HUSHEK S., MORIARTY T.: Cerebrovascular segmentation from ttf using stochastic models. *Medical Image Analysis* 10, 1 (Feb 2006), 2–18.
- [KAP02] KHOLMOVSKI E., ALEXANDER A., PARKER D.: Correction of slab boundary artifact using histogram matching. *Journal of Magnetic Resonance Imaging* 15 (2002), 610–617.
- [LXL00] LIU K., XU Y., LONCAR M.: Reduced slab boundary artifact in multi-slab 3d fast spin-echo imaging. *Magnetic Resonance in Medicine* 44 (2000), 269–276.
- [RSA\*04] REHM K., SCHAPER K., ANDERSON J., WOODS R., STOLTZNER S., ROTTENBERG D.: Putting our heads together: a consensus approach to brain/non-brain segmentation in t1-weighted mr volumes. *Neuroimage* 22, 3 (Jul 2004), 1262–1270.
- [SDB\*04] SEGONNE F., DALE A., BUSA E., GLESSNER M., SALAT D., HAHN H., FISCHL B.: A hybrid approach to the skull stripping problem in mri. *Neuroimage* 22, 3 (Jul 2004), 1060–1075.
- [SFF\*07] SAERING D., FIEHLER J., FORKERT N., PIENING M., HANDELS H.: Visualization and analysis of cerebral arterio-venous malformation combining 3d and 4d mr image sequences. *International Journal of Computer Assisted Radiology and Surgery* 2 (2007), 75–79.
- [SGBS00] STYNER M., GERIG G., BRECHBUEHLER C., SZEKELY G.: Parametric estimate of intensity inhomogeneities applied to mri. *IEEE Transaction On Medical Imaging* 19, 3 (2000), 153–165.
- [Smi02] SMITH S.: Fast robust automated brain extraction. *Human Brain Mapping* 17, 3 (2002), 143–155.
- [SSLS\*01] SHATTUCK D., SANDOR-LEAHY S., SCHAPER K., ROTTENBERG D., LEAHY R.: Magnetic resonance image tissue classification using a partial volume model. *Neuroimage* 13 (2001), 856–876.
- [Thi98] THIRION J.-P.: Image matching as a diffusion process: an analogy with maxwell’s demons. *Medical Image Analysis* 2, 3 (1998), 243–260.
- [WN99] WILSON D., NOBLE J.: An adaptive segmentation algorithm for time-of-flight mra data. *IEEE Transactions on Medical Imaging* 18, 10 (Oct 1999), 938–945.
- [WX01] WHITAKER R., XUE X.: Variable-conductance, level-set curvature for image denoising. *Proceeding of International Conference on Image Processing* 3 (2001), 142–145.